Extraction of resonance parameters from meson production reaction*

T. Sato[1,3;1)] N. Suzuki[1,3;2)] T. -S. H. Lee[2,3;3)]

1 (Department of Physics, Osaka University, Toyonaka, Osaka 560-0043, Japan)
2 (Physics Division, Argonne National Laboratory, Argonne, IL 60439, USA)
3 (Excited Baryon Analysis Center(EBAC), Thomas Jefferson National Accelerator Facility, Newport News, Virginia 23606, USA)

Abstract We have developed an analytic continuation method for extracting parameters of nucleon resonances within a Hamiltonian formulation of meson-nucleon reactions. The method was tested for simple solvable models and then applied for our recent coupled channels model (πN, ηN, $\pi\Delta$, ρN, and σN) of the πN and γ^*N reactions. The resonance pole positions and their properties are studied for P_{33} and P_{11} channels.

Key words baryon resonance, meson production reaction, resonance pole

PACS 13.75.Gx, 13.60.Le, 14.20.Gk

1 Introduction

The study of excited nucleon states (N*) has long been recognized as an important step towards developing a fundamental understanding of strong interactions. It is an important part of the effort to understand the structure of the nucleon since the dynamics governing the internal structure of composite particles, such as nuclei and baryons, is closely related to the structure of their excited states. Within the framework of Quantum Chromodynamics (QCD), a clear understanding of the spectrum and decay scheme of the N* states will reveal the role of confinement and chiral symmetry in the non-perturbative region.

The N* states are unstable and couple strongly with the meson-baryon continuum states to form nucleon resonances in meson production reactions on the nucleon. Therefore the extraction of nucleon resonance parameters from the reaction data is one of the important tasks in hadron physics[1, 2]. Ideally, the extraction of resonance parameter should involve the following step. (1) Perform complete measurement of all independent observables of the reactions considered. (2) Extract the partial wave amplitudes from the data. (3) Extract the resonance parameters from the extracted partial wave amplitudes. For the second step, we have developed a dynamical model for describing the extensive and high-quality data of πN and γ^*N reactions within a Hamiltonian formulation of multi-channels and multi-resonances reactions[3—9]. It includes πN, ηN and $\pi\pi$N channels, where the $\pi\pi$N channel is taken into account through the unstable particle channels ($\pi\Delta$, ρN, and σN). In this report we focus on the third step based on our recent work Ref. [10].

It will be useful to briefly recall how the resonance are defined[11—13]. By using analytic continuation, the scattering amplitude can be defined on the complex energy plane. The resonance is defined as a pole of the T-matrix on the unphysical energy sheet. The residue of the amplitude at the resonance pole gives a form factor of the resonance, which is the important information on the resonance structure. Comparing with the single channel case, the analytic structure of the amplitude becomes complex for the multi-channel

Received 7 August 2009

* Supported by Japan Society for the Promotion of Science, Grant-in-Aid for Scientific Research(C) 20540270, and U.S. Department of Energy, Office of Nuclear Physics Division, under contract No. DE-AC02-06CH11357, and Contract No. DE-AC05-060R23177 under which Jefferson Science Associates operates Jefferson Lab.

1) E-mail: tsato@phys.sci.osaka-u.ac.jp

2) E-mail: suzuki@kern.phys.sci.osaka-u.ac.jp

3) E-mail: lee@anl.gov

case as our interest on πN scattering. We have developed an analytic continuation method in order to extract resonance parameters from the scattering amplitude obtained from the dynamical coupled channel model of the meson production reaction. Our model of the meson production reaction is briefly summarized in section 2. Then we discuss the method to extract resonance pole from the amplitude in section 3. Here the main task is to handle the singularities associated with the unstable particle channels such as πΔ, ρN, and σN, which couple with the three-body ππN channel. The results from the application of the method for P_{11} and P_{33} πN amplitudes are shown in section 4. A brief summary is given in section 5.

2 Dynamical model for meson production reaction

The starting point of the dynamical model[4] for describing $\gamma N, \pi N \to$ MB reactions is the following Lippmann-Schwinger equation for the scattering T-matrix

$$T(E) = V + V\frac{1}{E - H_0 + i\epsilon}T(E). \quad (1)$$

The equation is coupled channel equation for the $N^* \oplus MB \oplus \pi\pi N$ model space. The interaction consists of the two-body meson-baryon and meson-meson interactions $v_{non-res}$, which are derived from the meson exchange model and the decay vertex Γ of $\rho, \sigma \to \pi\pi$ and $N^* \to M + B$ as

$$V = v_{non\text{-}res} + \Gamma + \Gamma^\dagger. \quad (2)$$

The interaction V is independent on the scattering energy and therefore the unitarity relation within the restricted Fock-space is trivially satisfied.

We rewrite Eq. (1) into a more convenient form for practical calculations. We achieve this rather complex task by applying the standard projection operator techniques, similar to that employed in a study of πNN scattering[14]. The details of our derivations are given in Appendix B of Ref. [4]. The resulting MB → M′B′ amplitude in each partial wave consists of a non-resonant amplitude $t^{non-res}(E)$ and a resonant amplitude $t^{res}(E)$ as illustrated in Figs. 1 and 2. It can be written as

$$T(E) = t^{non\text{-}res}(E) + t^{res}(E). \quad (3)$$

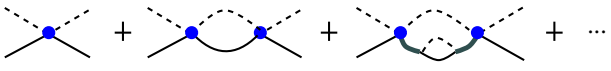

Fig. 1. Graphical representation of the non-resonant amplitude

The non-resonant amplitude $t^{non-res}$ is obtained by solving the following coupled-channel integral equations

$$t^{non\text{-}res}(E) = v^{non\text{-}res} + v^{non\text{-}res} G_{MB}(E) t^{non\text{-}res}(E). \quad (4)$$

The meson-baryon propagator G_{MB} in Eq. (4) takes the following form

$$G_{MB}(E) = \frac{1}{E - E_B - E_M - \Sigma_{MB}(E) + i\epsilon}, \quad (5)$$

where E_B and E_M are energies of baryon and meson on the mass-shell. The mass shift $\Sigma_{MB}(E)$ depends on the considered MB channel. It is $\Sigma_{MB}(E) = 0$ for the stable particle channels (MB = πN, ηN). For channels containing an unstable particle, such as MB = πΔ, ρN, σN, Σ_{MB} is self-energy of the unstable particle with a spectator pion as illustrated in the third diagram of Fig. 1 as

$$\Sigma_{MB}(E) = \langle MB | \Gamma \frac{1}{E - E_\pi - E_\pi - E_N + i\epsilon} \Gamma^\dagger | MB \rangle. \quad (6)$$

Fig. 2. Graphical representation of the resonant amplitude.

The resonant term T^{res} is defined by

$$t^{res}(E) = \sum_{N_i^*, N_j^*} \bar{\Gamma}_{N_i^* \to M'B'}(E) [D(E)]_{i,j} \bar{\Gamma}_{MB \to N_j^*}(E), \quad (7)$$

with the N∗ Green's function given as

$$[D(E)^{-1}]_{i,j}(E) = (E - M^0_{N_i^*})\delta_{i,j} - \bar{\Sigma}_{i,j}(E). \quad (8)$$

$M^0_{N^*}$ is the mass of a bare N^* state, and the self-energies are

$$\bar{\Sigma}_{i,j}(E) = \sum_{MB} \bar{\Gamma}_{MB \to N_i^*}(E) G_{MB}(E) \Gamma_{N_j^* \to MB}. \quad (9)$$

In general, the bare states mix with each other through the off-diagonal matrix elements of the self-energies. The dressed vertex interactions in Eq. (7) and Eq. (9) are

$$\bar{\Gamma}_{MB \to N^*}(E) = \Gamma_{MB \to N^*} + \sum_{M'B'} \Gamma_{M'B' \to N^*} \times G_{M'B'}(E) t^{non\text{-}res}(E). \quad (10)$$

The scattering amplitudes are solved for real energy E for the observables of πN reactions, while in order to investigate the resonance pole from the above amplitude, one has to solve the above equations for complex energy E and analytic continue the amplitude on the unphysical sheet.

3 Analytic continuation of the scattering amplitude

For resonance search, we solve the coupled channel equation Eq. (1) for complex energy. Therefore, a numerical method for analytic continuation of the amplitudes has to be developed. A key for selecting the amplitude on physical sheet or unphysical sheet is how to include the singularities of the meson-baryon Green functions $G_{\rm MB}$. The meson-baryon Green function appears in the Lippmann-Schwinger equation for the non-resonant T-matrix

$$t^{\text{non-res}}(p',p;E)=v(p',p)+\int_{\rm C}{\rm d}q\,q^2v(p',q)G_{\rm MB}(E,q)t^{\text{non-res}}(q,p;E), \quad (11)$$

and the self-energy of $\rm N^*$

$$\bar{\Sigma}_{i,j}(E)=\sum_{\rm MB}\int_{\rm C}{\rm d}qq^2\bar{\Gamma}_{{\rm MB}\to{\rm N}^*_i}(E,q)\times G_{\rm MB}(E,q)\Gamma_{{\rm N}^*_j\to{\rm MB}}(q). \quad (12)$$

The choice of the integration path C will be discussed later in this section.

For multi-channel case, the unphysical sheets can be specified by physical or unphysical sheets for each meson-baryon channels, where at least one of the channels should be on the unphysical sheet. In general there can be many poles associated with single resonance and the pole which is nearest to the physical sheet is supposed to play a dominant role. In our numerical study, we search for the poles close to the physical sheet.

3.1 Channel with stable particles

For channel with stable particles, the meson-baryon Green function is given as

$$G_{\rm MB}(E,q)=\frac{1}{E-E_{\rm M}(q)-E_{\rm B}(q)}. \quad (13)$$

The Green function has a pole at $q=p_0$ given as

$$E=\sqrt{m_{\rm M}^2+p_0^2}+\sqrt{m_{\rm B}^2+p_0^2}. \quad (14)$$

The physical scattering amplitude at a positive energy E can be obtained from Eq. (11) by setting $E\to E+{\rm i}\epsilon$ with a positive $\epsilon\to 0$ and choosing the integration contour C to be along the real-axis of p with $0\leqslant p\leqslant\infty$. From Eq. (11) it is clear that $t^{\text{non-res}}(E)$ has a discontinuity on the positive real E

$${\rm Dis}(t(E))=t(E+{\rm i}\epsilon)-t(E-{\rm i}\epsilon)=2\pi{\rm i}\rho(p_0)v(p_0,p_0)t(E), \quad (15)$$

where $\rho(p_0)=p_0E_1(p_0)E_2(p_0)/E$. Thus the t-matrix has a cut running along the real positive E.

The resonance poles can be found from $T(E)$ on the unphysical Riemann sheet. To find resonance poles with the energy above MB-threshold, we need to find a solution of Eq. (11) on the unphysical sheet. The pole p_0 of the propagator is on the lower p-plane, as shown in Fig. 3(a). It is well-known[15—18] the analytic continuation of the solution on the unphysical sheet is achieved by deforming the integration path as contour $\rm C_1'$ shown in Fig. 3(a). By this the pole will not cross the cut and the integral is analytically continued from real positive E to the lower half of the unphysical E-sheet with ${\rm Im}(p_0)\leqslant 0$. Obviously, the same solution can be obtained by choosing any contour which is below the pole position p_0, such as the contour $\rm C_1$ in Fig. 3(b).

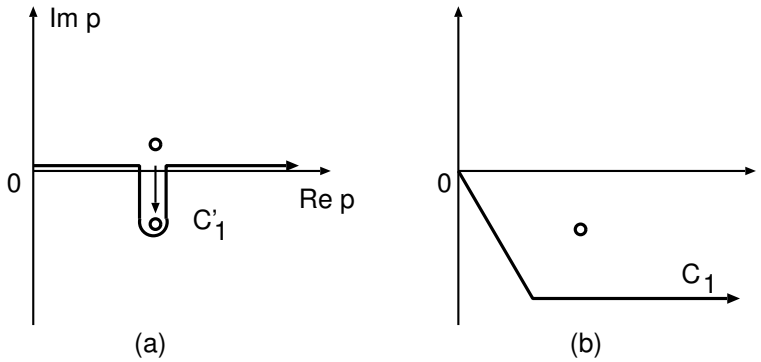

Fig. 3. The shift of the singularity (open circle) of the propagator of the two-particle scattering equation as energy E moves from real value to negative imaginary. $\rm C_1'$ in (a) or $\rm C_1$ in (b) is the integration path for calculating the scattering amplitude with E on the unphysical plane.

It is noticed that we have assumed the potential $v(p',p)$ is analytic in the region we have deformed the path.

3.2 Channel including unstable particle

For meson-baryon reactions, the nucleon resonances can decay into some unstable particle channels such as the $\pi\Delta$, ρN, σN considered in the model of Ref. [4]. Here we discuss an analytic continuation method to find resonance poles for such a reaction model.

Here we examine $\pi\Delta$ channel as an example. The meson baryon Green function $G_{\rm MB}$ is given as

$$G_{\pi\Delta}(E,p) = \frac{1}{E - E_\pi(p) - E_\Delta(p) - \Sigma_\Delta(E,p)}, \quad (16)$$

where

$$\Sigma_\Delta(p,E) = \int_{C_3} \frac{\{g_{\Delta,\pi N}(q)\}^2 q^2 dq}{E - E_\pi(p) - [(E_\pi(q) + E_N(q))^2 + p^2]^{1/2}}. \quad (17)$$

At first we examine the analytic structure of $G_{\pi\Delta}$. The $\pi\Delta$ Green function has singularities associated with the $\pi\pi$N and the "$\pi\Delta$ continuum" in complex E plane as indicated by dashed lines in Fig. 4.

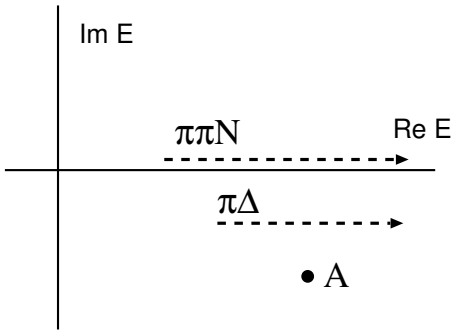

Fig. 4. Singularity of the $\pi\Delta$ Green function.

The analytic continuation of the scattering amplitude for $\pi\Delta$ channel can be done by choosing the appropriate contour C of Eqs. (11) and (12). For given real E, the discontinuity of the $\pi\Delta$ propagator is the $\pi\pi$N cut along the real axis between $\pm p_0$ ($-p_0 \leqslant p \leqslant p_0$) which is obtained by solving

$$E = E_\pi(p_0) + [(m_\pi + m_N)^2 + p_0^2]^{1/2}. \quad (18)$$

There is also a singularity at momentum $p = p_x$, which satisfies

$$E - E_\pi(p_x) - E_\Delta(p_x) - \Sigma_\Delta(p_x, E) = 0. \quad (19)$$

Physically, this singularity corresponds to the $\pi\Delta$ two-body scattering state.

As an example, for finding the resonance pole with $\mathrm{Re}(E) > m_\pi + m_\Delta$ and $\mathrm{Im}(E) < \mathrm{Im}(M_\Delta)$ shown as point A in Fig. 4, the integration contour of momentum p must be chosen to stay below the $\pi\pi$N cut (dashed line) and the singularity p_x, such as the contour C_2 shown in Fig. 5. It is noticed further that the singularity position q_0 of the propagator in Eq. (17) depends on spectator momentum p

$$E - E_\pi(p) = [(E_\pi(q_0) + E_N(q_0))^2 + p^2]^{1/2}. \quad (20)$$

Therefore the singularity q_0 moves when the momentum p varies along the path C_2 of Fig. 5. The integration contour C_3 of Eq. (17) controls physical or unphysical sheet of $\pi\pi$N channel.

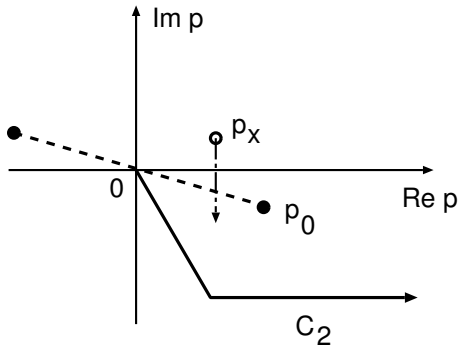

Fig. 5. Contour C_2 for calculating the $\pi\Delta$ self-energy on the unphysical sheet.

3.3 Toy model

To illustrate how the procedure of the analytic continuation in the previous sections works, we examined a simple toy model. The model consists of N*, $\pi\Delta$ and $\pi\pi$N Fock space. The N* couple with $\pi\Delta$ channel and the $\pi\Delta$ state decays into into $\pi\pi$N. The resonance pole is given by solving

$$M_{N^*} = m_0 + \Sigma_{\pi\Delta}(M_N^*) \quad (21)$$

with

$$\Sigma_{\pi\Delta} = \int dp p^2 [g_{N^*\pi\Delta}(p)]^2 G_{\pi\Delta}(W,p). \quad (22)$$

The $\pi\Delta$ Green's function is given in Eq. (16). Eq. (21) corresponds to a condition for a pole of $T^{\rm Res}$ (Eq. (7)), which is equivalent to finding a pole of N* Green function (Eq. (8)). In this simple model, the non-resonant interactions and the coupling of N* with MB channels other than $\pi\Delta$ channel are turned off. We take a non-relativistic kinetic energies of mesons and baryons, the s-wave interaction with mono pole vertex form factors. This model enables us to obtain semi-analytic results, which can be used to test the contour deformation method for analytic continuation.

We have studied the resonance pole by increasing the strength of $N^* \to \pi\Delta$ coupling constant. For vanishing coupling constant the resonance pole is at

$M_{N^*} = m_0$ as shown in Fig. 6. Increasing $g_{N^*\pi\Delta}$, the trajectory of the resonance pole is shown in Fig. 6. The pole moves below $\pi\Delta$ cut on the $\pi\Delta$ unphysical sheet. Further increasing the $g_{N^*\pi\Delta}$, the width of the resonance becomes smaller because of the decreasing the available phase space for N^* decay. The width remains finite when $\mathrm{Re}(M^*_N)$ moves below the $\pi\Delta$ threshold, since the width of the resonance is due to the decay of N^* into $\pi\pi N$. Finally the resonance becomes a bound state of $\pi\pi N$ system. In all case the pole positions of the contour deformation method agree with those of the semi-analytic calculation.

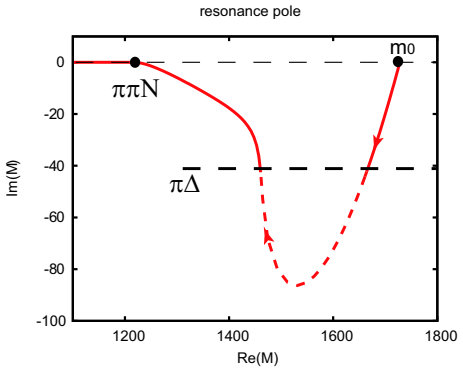

Fig. 6. Trajectory of the resonance pole.

4 Resonance poles of P_{11} and P_{33}

We apply the method of analytic continuation to our dynamical coupled-channel model developed in Ref. [5]. The model gives a good description of the πN elastic scattering, pion photoproduction[8], $(\pi,\pi\pi)$[6] and single pion electroproduction reactions[9].

Here we show the results on P_{33} and P_{11} resonances. In both channels, the non-resonant T-matrix $T^{\text{non-res}}$ does not have a pole and the resonance poles are on the resonant amplitude T^{res}. We list the poles near to the physical sheet.

The resonance amplitude is parametrized as

$$T = \frac{\mathrm{Re}^{i\theta}}{E - M_{\text{res}}}. \quad (23)$$

Our results on the resonance pole and residue for P_{33} channel is listed in Table 1. Our results agree well with those of the other studies.

Table 1. Parameters of P_{33} resonance.

analysis	M_Δ/MeV	residue (R/MeV, θ°)
this work	(1211,−50)	(52, −46)
GWU/VPI[19]	(1211, −50)	(52, −47)
Jülich Model[20]	(1218, −45)	(47, −37)
Höhler[21]	(1209, −50)	(50, −48)
Cutkosky[22]	(1210, −50)	(53, −47)

For P_{11} channel, we focus on the three poles we found in the model. We found poles at $M_{N^*} = 1820 - 248\mathrm{i}(\mathrm{A}),\ 1357 - 76\mathrm{i}(\mathrm{B}),\ 1364 - 105\mathrm{i}(\mathrm{C})$. The almost degenerate two poles around $\pi\Delta$ threshold are also found in recent works from Jülich and GWU/VPI as shown in Table 2. We can examine how those resonances develop from the 'bare' N^* though the coupled channel dynamics. For this purpose, we artificially modified the Green function in Eq. (8) by introducing a scale factor y for the N^* self energy as

$$[D(E)^{-1}]_{ij}(E) = (E - M^0_{N^*_j})\delta_{ij} - y\bar{\Sigma}_{ij}(E). \quad (24)$$

By increasing y from zero, we can examine the evolution of the resonance poles as shown in Fig. 7. The dotted curve shows how 'bare' resonance moves to resonance pole A. The resonance A is above the threshold energy of ηN and $\pi\Delta$ and it is on the unphysical sheet of both channels. The dashed curve shows how the same "bare" state evolves on the ηN physical sheet. Here we have switched off the coupling of N^* with $\pi\Delta$ channel for the dashed line. The real part of the pole reaches around 1400 MeV below ηN threshold. We then turn on the coupling with $\pi\Delta$ channel and the resonance split into resonance B(C) on the $\pi\Delta$ unphysical (physical) sheet. Within the dynamical model, it is shown the three resonance poles are evolved from the same bare state. This finding indicates there is a possibility that poles of the resonances may not belongs to the different core states such as predicted from constituent quark model but one core state can evolve dynamically into several poles.

Table 2. P_{11} resonance poles near the Roper resonance position of PDG.

analysis	P_{11} poles/MeV	
this work	(1357, −76)	(1364, −105)
GWU/VPI[19]	(1359, −82)	(1388, −83)
Jülich Model[20]	(1387, −74)	(1387, −71)

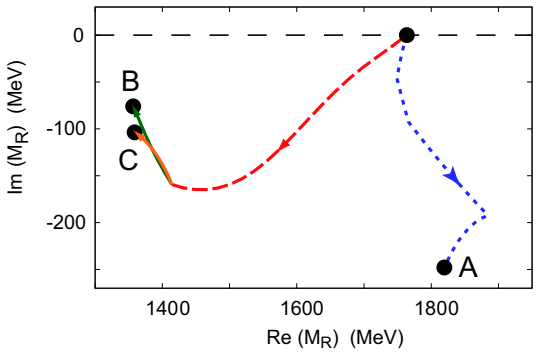

Fig. 7. Trajectory of P_{11} resonance pole.

5 Summary

We have developed a method of analytic continuation of the scattering amplitude within the dynamical coupled channel reaction model. The resonance information can be extracted from the amplitude on the unphysical energy plane using the method. As an example, we have shown the poles of the P_{11} and P_{33} amplitudes using the realistic model of the pion-nucleon scattering. We found three pole of P_{11} channel are associated to the single bare resonance state. Extension of the method to extract electromagnetic resonance form factor is in progress.

References

1 Burkert V, Lee T -S H. Int. J. Mod. Phys. E, 2004, **13**:1035
2 Sato T, Lee T -S H. J. Phys. G, 2009, **36**: 073001
3 Sato T, Lee T -S H. Phys. Rev C, 1996, **54**: 2660
4 Matsuyama A, Sato T, Lee T -S H, Phys. Rept., 2007 **439**: 193
5 Julia-Diaz B, Lee T -S H, Matsuyama A, Sato T. Phys. Rev. C, 2007, **76**: 065201
6 Kamano H, Julia-Diaz B, Lee T -S H, Matsuyama A, Sato T. Phys. Rev. C, 2009, **79**: 025206
7 Durand J, Julia-Diaz B, Lee T -S H, Saghai B, Sato T. Phys. Rev. C, 2008, **78**: 025204
8 Julia-Diaz B, Lee T -S H, Matsuyama A, Sato T, Smith L C. Phys. Rev. C, 2008, **77**:045205
9 Julia-Diaz B, Kamano H, Lee T -S H, Matsuyama A, Sato T, Suzuki, N. Phys. Rev. C, 2009, **80**: 025207
10 Suzuki N, Sato T, Lee T -S H. Phys. Rev. C, 2009, **79**: 025205
11 Newton R G. Scattering Theory of Waves and Particles. New York: Springer-Verlag, 1982
12 Taylor J R. Scattering Theoy. New York: John Wiley and Sons, 1972
13 Goldberger M L, Watson K M. Collision Theory, Robert E. Krieger Publishing Company, INC. 1975
14 Lee T-S H, Matsuyama A. Phys. Rev. C, 1985, **32**: 516
15 Badalyan A M, Kok L P, Polikarpov M I, Simonov Yu A. Phys. Rept., 1982, **82**: 31
16 Orlov Yu V, Turovtsev V V. Sov. Phys. JETP, 1989, **59**: 902
17 Pearce B C, AfnanI R. Phys. Rev. C, 1984, **30**: 2022
18 Pearce B C, Gibson B F. Phys. Rev. C, 1989, **40**: 902
19 Arndt R A, Briscoe W J, Strakovsky I I, Workman R L. Phys. Rev C, 2006, **74**: 045205
20 Döring M, Hanhardt C, Huang F, Krewald S, Meißner U -G. arXiv:0903.1781 [nucl-th]; Döring M, Hanhardt C, Huang F, Krewald S, Meißner U -G. arXiv:0903.4337 [nucl-th]
21 Höhler G. πN Newsletter, 1993, **9**: 1
22 Cutkosky R E, Forsyth C P, Hendrick R E, Kelly R L. Phys. Rev. D, 1979, **20**: 2839